Solid-State NMR and X-ray Diffraction Studies of the Geometry and Intramolecular Dynamics of Bis(organothiophosphoryl) Dichalcogenides

Marek J. Potrzebowski,*,† Jaroslaw Blaszczyk,‡ Michal W. Wieczorek,‡ and Jacek Klinowski*,§

Centre of Molecular and Macromolecular Studies, Polish Academy of Sciences, Sienkiewicza 112, 90-362 Lódz, Poland, Institute of Technical Biochemistry, Technical University of Lódz, Stefanowskiego 4/10, 90−924 Lódz, Poland, and Department of Chemistry, University of Cambridge, Lensfield Road, Cambridge CB2 1EW, U.K.

Received: December 4, 1996; In Final Form: July 14, 1997[⊗]

Information stored in the Cambridge Crystallographic Data Centre shows that *anti*−*anti* conformation is common for bis(organothiophosphoryl) dichalcogenides. In view of the 1−4 repulsion, the *syn*−*syn* conformation of the $S^1{=}P{-}X{-}X^4{-}P{=}S$ (X = S and Se) backbone is unfavorable. However, in compounds with at least one phenyl group directly bonded to the phosphorus, such as bis[*tert*-butyl(phenyl)thiophosphinyl] disulfide (Knopik, P. et al. *J. Chem. Soc., Dalton Trans.* **1993**, 2749), bis(diphenylthiophosphinyl) disulfide (Gallacher, A. C. et al. *Acta Crystallogr.* **1993**, *C49*, 1793) and bis[*tert*-butyl(phenyl)thiophosphinyl] diselenide (this work) there is the *syn*−*syn* geometry caused by the aromatic−aromatic interactions. Bis[*tert*-butyl-(phenyl)thiophosphinyl] diselenide is monoclinic, space group $C2/c$ with $a = 20.424(2)$ Å, $b = 9.373(1)$ Å, $c = 12.907(1)$ Å, $V = 2406.4(2)$ Å^3, $D_c = 1.525$ (2) g/cm^3, and $Z = 4$. Refinement using 2351 reflections for 118 variables gives $R = 0.047$. We have used high-resolution ^{77}Se MAS NMR to study the structural properties of the compound. The principal elements T_{ii} of the ^{77}Se effective dipolar/chemical shift tensor were calculated from the intensities of the spinning sidebands. The values of the anisotropy and asymmetry parameters reflect the distortion of the environment of selenium. For a series of bis(organothiophosphoryl) diselenides the T_{33} tensor component gives the largest contribution to the isotropic chemical shifts and the span parameter Ω reflects the strength of the diselenide bond. Molecular packing significantly influences the intramolecular dynamics of the aliphatic and aromatic groups. The ^{13}C dipolar dephasing experiment and line shape analysis of the ^{1}H−^{2}H CP/MAS spectra of selectively ^{2}H-labeled compounds show that the phenyl groups are static as a result of the aromatic−aromatic interaction, while the *tert*-butyl groups are under a fast motional regime, with C_{3v} jumps around the P−C and C−C bonds.

Introduction

Strong attractive interactions between π-systems[1] control the packing of aromatic molecules in crystals,[2] tertiary structures of proteins,[3] complexation in many host−guest systems,[4] and the stereochemistry of organic reactions[5] and stabilize the double helical structure of DNA.[6] Interactions between aromatic rings also play a significant role in supramolecular chemistry and crystal engineering.[7] The aromatic−aromatic interactions involve mainly the two extremes, the $\pi-\pi$ stacking of parallel-shifted ("face-to-face") aromatic rings and the T-shaped ("edge-to-face") configuration in which the C−H dipoles at the rim of one ring point toward the negatively charged carbons of the second ring.[8,9] Hunter and Sanders proposed an electrostatic model to account for the influence of electronic factors on π-stacking,[10] while Cozzi and Siegel introduced the term "polar/π" to emphasize the polar character of the interactions between aromatic rings.[11−13] We use the charge distribution model of a π-system to rationalize the geometry of bis[*tert*-butyl(phenyl)-thiophosphinyl] diselenide **1** and bis[*tert*-butyl(phenyl)thiophosphinyl] disulfide **2**.

Bis(organothiophosphoryl) dichalcogenides are useful model compounds for the study of the structure and dynamics of solid organophosphorus compounds and aid the understanding of the nature of the S−S and Se−Se bonds.[14−20] In view of the significance of the disulfide bonds in the chemistry of natural products, compounds with an S−S linkage have received much attention.[21,22] In an unstrained molecular environment the C−S−S−C torsional angle is 80−85° both in the liquid and the solid state. By contrast, bis(organothiophosphoryl) dichalcogenides easily form a conformation with the P−X−X−P (X = S and Se) torsional angle of 180°. Moreover, the S=P−X−X−P=S unit adopts planar zigzag geometry with the *anti*−*anti*, *anti*-*syn*, and *syn*−*syn* arrangement (Scheme 1).

SCHEME 1

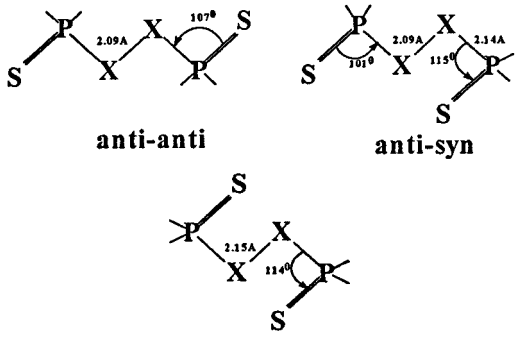

Electronic effects, such as the overlap between the p orbital of sulfur or selenium and the d_{xz} or d_{yz} orbitals of phosphorus, are responsible for the planar geometry.[20,23] The *anti*−*anti* conformation is common in bis(organothiophosphoryl) dichalcogenides,[24] and only a handful of X-ray structures with *syn*−*syn* geometry,[23] e.g., bis(diphenylthiophosphinyl) disulfide[25] and

† Polish Academy of Sciences.
‡ Technical University of Lódz.
§ University of Cambridge. Telephone: +(44)-1223−33 65 14. FAX: +(44)-1223-33 63 62. E-mail: jk18@cam.ac.uk.
⊗ Abstract published in *Advance ACS Abstracts,* September 15, 1997.

S1089-5647(96)03976-4 CCC: $14.00

bis[*tert*-butyl(phenyl)thiophosphinyl] disulfide,[20] have been reported. Since both compounds have at least one phenyl group directly bonded to phosphorus, we assume that the aromatic−aromatic interaction is the driving force toward the *syn*−*syn* geometry.

We have studied the influence of the $\pi-\pi$ interaction on molecular structure, molecular packing and dynamics of aliphatic/aromatic groups bonded to phosphorus for diselenide **1** and disulfide **2** using ^{2}H, ^{13}C, ^{31}P, and ^{77}Se solid-state NMR and X-ray diffraction (XRD), and we examine the relationship between the local geometry of phosphorus and selenium and the ^{31}P and ^{77}Se NMR chemical shift parameters.

Experimental Section

NMR Measurements. CP/MAS NMR spectra were recorded with high-power (1.05 mT) proton decoupling on a Bruker MSL-300 spectrometer at 46.07 MHz for ^{2}H, 75.46 MHz for ^{13}C, 121.46 MHz for ^{31}P, and 57.21 MHz for ^{77}Se. Powdered samples were spun in cylindrical MAS rotors at 2.0−4.5 kHz. In the $^{1}H-^{2}H$ experiments, the contact time was 7 ms, the spectral width 250 kHz, and repetition time 10 s. Each spectrum represents 8000 data points. The Bloch decay ^{2}H MAS spectra were recorded with 90° pulse of 3.5 μs and repetition time 6−100 s. In the ^{13}C experiments, the contact time was 5 ms, the repetition time 6 s, and the spectral width 20 kHz. The 8000 data points were accumulated with a total of 100−200 scans. ^{13}C chemical shifts are given in ppm from tetramethylsilane (TMS) and were measured indirectly by reference to the glycine carbonyl peak at 176.3 ppm relative to tetramethylsilane. In the ^{31}P experiments, the contact time was 5 ms, the repetition time 6 s, and the spectral width 50 kHz. The 8000 data points were accumulated with a total of 100 scans. The ^{31}P chemical shifts were measured indirectly using bis(dineopentoxythiophosphoryl) disulfide set at 84.0 ppm from 85% H_3PO_4. The $^{1}H-^{77}Se$ Hartmann−Hahn condition for CP/MAS experiments was set up using powdered ammonium selenate. The contact time was 5 ms, the repetition time 10 s, and the spectral width 50 kHz. The spectrum of diselenide **1** was accumulated 12 000 times in order to achieve a reasonable signal-to-noise ratio. The ^{77}Se chemical shifts were measured indirectly by reference to ammonium selenate set at 1040.2 ppm from Me_2Se.

The principal components of the ^{31}P chemical shift tensor and shielding parameters were calculated using the WIN-MAS program.[26−28] The principal components δ_{ii} were used for calculation of the chemical shift parameters, anisotropy $\Delta\delta$, asymmetry η, span Ω, and skew κ.[29]

If

$$|\delta_{11} - \delta_{iso}| > |\delta_{33} - \delta_{iso}|$$

then

$$\Delta\delta = \delta_{11} - (\delta_{22} + \delta_{33})/2 \quad (1)$$

$$\eta = (\delta_{22} - \delta_{33})/(\delta_{11} - \delta_{iso}) \quad (2)$$

If

$$|\delta_{11} - \delta_{iso}| < |\delta_{33} - \delta_{iso}| \text{ and } \delta_{11} > \delta_{22} > \delta_{33}$$

then

$$\Delta\delta = \delta_{33} - (\delta_{11} + \delta_{22})/2 \quad (3)$$

$$\eta = (\delta_{22} - \delta_{11})/(\delta_{33} - \delta_{iso}) \quad (4)$$

Moreover, we have

$$\Omega = \delta_{11} - \delta_{33} \quad (5)$$

$$\kappa = (3(\delta_{22} - \delta_{iso}))/\Omega \quad (6)$$

X-ray Crystallography. The crystal and molecular structure of **1** was determined using data collected on a CAD4 diffractometer.[30] Compound **1** crystallized in the monoclinic system, space group *C*2/*c*. Intensity data were collected at room temperature using graphite-monochromated Cu Kα radiation. Lattice constants were refined by a least-squares fit of 25 reflections in the θ range of 20.1−29.7°. The decline in intensities of the three standard reflections, (2, −4, 4), (−7, −3, 3), and (−4, −4, −1), was 2.1% during 27.7 h of exposure, and all measured intensities were corrected using the DECAY program. Empirical absorption correction was applied using the ψ scan method.[31,32] A total of 2352 observed reflections with $I \geq 3\sigma(I)$ were used to solve the structure by direct methods and to refine it by full matrix least-squares using F's. Scattering factors were taken from the *International Tables for X-ray Crystallography*.[33] Hydrogen atoms were placed at idealized positions and set as riding, with fixed isotropic thermal parameters. Anisotropic thermal parameters were refined for all non-hydrogen atoms. The final refinement converged to $R = 0.047$ with unit weight for 118 refined parameters. Supplementary data for this structure can be obtained from the Cambridge Crystallographic Data Centre.[34]

Results and Discussion

Structure of Bis[*tert*-butyl(phenyl)thiophosphinyl] Diselenide. The proton-decoupled room-temperature ^{31}P CP/MAS spectrum of bis[*tert*-butyl(phenyl)thiophosphinyl] diselenide **1** (Figure 1a) contains a set of spinning sidebands caused by the large chemical shielding anisotropy (CSA). The principal components of the ^{31}P chemical shift tensor were calculated from the intensities of the spinning sidebands using the WIN-MAS program based on the Berger−Herzfeld algorithm (Table 1).[27,28]

The ^{31}P chemical shift parameters can be correlated with the molecular structure of the S═P−S−S−P═S unit,[15,19] and we have found a linear relationship between the anisotropy $\Delta\delta$, asymmetry η, and the S═P−S angles. Replacement of sulfur by selenium in the S═P−X−X−P═S unit has little influence on the shielding parameters ($\Delta\delta$, η, Ω, and κ) if the geometry is unchanged.[17] Important structural information can thus be obtained by comparing ^{31}P chemical shift parameters of bis[*tert*-butyl(phenyl)thiophosphinyl] diselenide **1** with those of disulfide **2**, the molecular structure of which is known.[20]

Similar values of parameters Ω and κ for diselenide **1** and disulfide **2** suggest that the molecular structure of these compounds is very similar. The Ω values in the range 255−265 ppm are larger than in other bis(organothiophosphoryl) dichalcogenides and indicate that the S═P−Se and S═P−S valence angles are 114−117°. The distortion of S═P−X angle from tetrahedral is characteristic for the *syn* geometry. The values of ^{31}P chemical shift parameters show that the molecular structure of **1** is very similar to that of **2**. A comparison of ^{31}P CP/MAS spectra of **1** (Figure 1a) and **2** (Figure 1b) provides further support for this conclusion.

Figure 1a indicates that diselenide **1** exists as two polymorphs; the main product as a single resonance at 91.3 ppm and traces of the second component (marked with asterisks) at 99.2 ppm. By analogy with the disulfide **2**, it is assumed that the major polymorph of compound **1** crystallizes in a space group in which

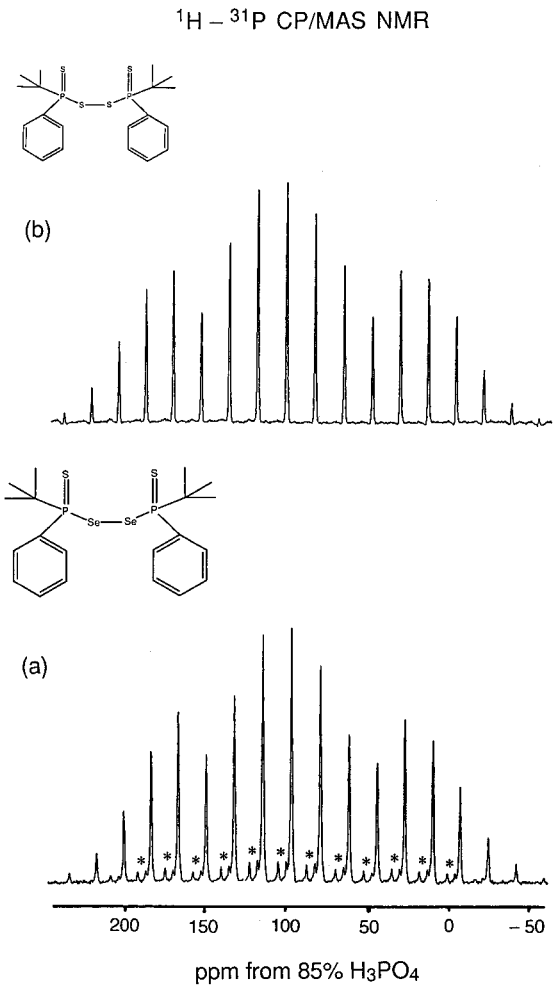

Figure 1. ^{1}H−^{31}P CP/MAS spectra of (a) bis[*tert*-butyl(phenyl)-thiophosphinyl] diselenide **1** and (b) bis[*tert*-butyl(phenyl)thiophosphinyl] disulfide **2**. Lines from the second polymorph of diselenide **1** are marked with asterisks. Each spectrum has 8000 data points, a contact time of 5 ms, and 100 scans.

TABLE 1: ^{31}P Chemical Shift Parameters for Bis[*tert*-butyl(phenyl)thiophosphinyl] Diselenide 1 and Bis[*tert*-butyl(phenyl)thiophosphinyl] Disulfide 2[a]

compound	δ_{iso} (ppm)	δ_{11} (ppm)	δ_{22} (ppm)	δ_{33} (ppm)	$\lvert\Delta\delta\rvert$ (ppm)	Ω (ppm)	η	κ
diselenide **1**	91.3	212	100	−36	192	248	0.88	0.11
disulfide **2**	102.1	224	110	−30	197	254	0.88	0.09

[a] Estimated errors in δ_{11}, δ_{22}, δ_{33}, and $\Delta\delta$ are ±5 ppm; errors in δ_{iso} are ±0.2 ppm. Principal components of the chemical shift tensor are defined as $\delta_{11} > \delta_{22} > \delta_{33}$. Isotropic chemical shift is given by $\delta_{iso} = (\delta_{11} + \delta_{22} + \delta_{33})/3$.

half of the molecule is the asymmetric part of the unit cell, and the *C*2/*c* space group is the most likely. Since the resonance lines are broadened at the base, indirect spin−spin coupling constants between ^{31}P and ^{77}Se, expected to be ca. 400−500 Hz, could not be measured. We were also unable to obtain the second polymorph in a yield larger than a few percent. On the strength of the ^{31}P CP/MAS spectrum we suggest that the two resonances in the isotropic part of the spectrum for the second crystallographic form of diselenide **1** correspond to a space group in which the whole molecule is the asymmetric unit.

^{77}Se CP/MAS spectra can provide additional structural information on the local environment of selenium, as the anisotropic shielding of ^{77}Se is highly sensitive to even small departures from spherical symmetry.[17,35] For lower symmetry environments the large anisotropy leads to large number of

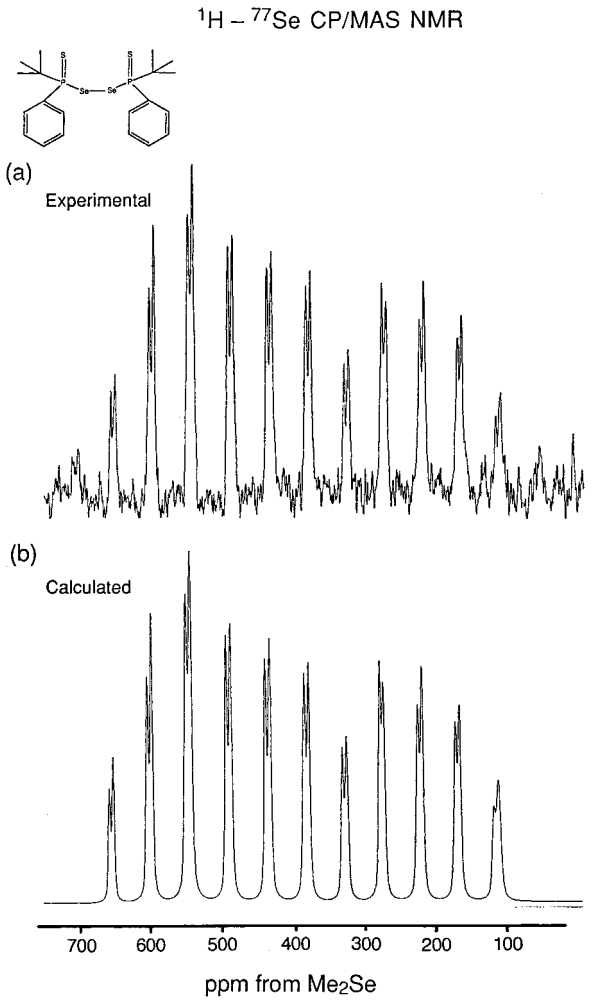

Figure 2. (a) ^{1}H−^{77}Se CP/MAS spectrum of diselenide **1** acquired at 57.21 MHz. The spectrum has 12 000 data points with 10 Hz line broadening, a contact time of 5 ms, and 2000 scans and $\nu_{rot} = 3.2$ kHz. (b) Spectrum calculated using the WIN-MAS program.

spinning sidebands. In the case of P−Se systems, for isolated $I = {}^1/_2$ spin pairs ^{31}P−^{77}Se, the spin−spin and dipolar interactions must be taken into account. Since the ^{77}Se CP/MAS spectrum of bis[*tert*-butyl(phenyl)thiophosphinyl] diselenide **1** (Figure 2a) is very broad (over 30 kHz), it is clear that under slow rotation the chemical shift is not averaged to the isotropic value.

Following Zilm and Grant[36] we denote the effective dipolar/chemical shift tensor by $\mathbf{T}_{ii}$. Analysis of sideband intensities gives the principal values of the tensors $\mathbf{T}_{ii+}$ and $\mathbf{T}_{ii-}$. The values of δ_{iso} and of the isotropic coupling constant $^1J_{(31P-77Se)}$ can be obtained directly. The calculated values of the principal tensor components for ^{77}Se, the anisotropy parameter, span, asymmetry, and skew are given in Table 2. The calculated spectrum is shown in Figure 2b.

A comparison of the geometric parameters for diselenide **1** with those for bis(diisopropoxythiophosphoryl) diselenide **3**,[37] bis(dineopentoxythiophosphoryl) diselenide **4**[37] and bis(5,5-dimethyl-2-thiono-1,3,2-dioxaphosphorinane-2-yl) diselenide **5**[16] shows that the Se−Se bond lengths are correlated with the P−Se−Se−P torsional angle. For compound **1** this angle is 92° and the Se−Se bond length 2.277(1) Å, for **3** and **4** the torsional angles are 180.0°, the Se−Se distances 2.376(1) and 2.381(1) Å, and for **5** 118.7° and 2.329(1) Å, respectively. The shortest Se−Se bonds are associated with the P−Se−Se−P angle close to 90° which gives the maximum overlap between the lone electron pair and the S_{P-Se} orbital. This stereoelectronic

TABLE 2: ^{77}Se Chemical Shift Parameters and Selected Geometrical Parameters for Diselenides 1 (this work), 3 and 4 (Reference 37), and 5 (Reference 16)[a]

diselenide	Se−Se bond lengths (Å)	P−Se bond lengths (Å)	conformation (torsional angle)	spin	T_{11} (ppm)	T_{22} (ppm)	T_{33} (ppm)	ΔT (ppm)	Ω (ppm)	η	κ	δ_{iso} (ppm)
1	2.277(1)	2.299(2)	P−Se−Se−P = 92.0°	A^-	734	532	114	520	620	0.58	0.35	459.9
				A^+	709	555	98	534	611	0.43	0.50	453.7
3	2.376(1)	2.218(1)	P−Se−Se−P = 180.0°	A^-	660	365	−149	664	809	0.68	0.27	293.0
				A^+	656	336	−171	620	827	0.75	0.19	283.7
4	2.381(1)	2.230(2)	P−Se−Se−P = 180.0°	A^-	617	393	−169	−674	785	0.50	0.43	280.2
		2.223(2)		B^-	609	404	−178	−683	787	0.45	0.55	278.3
				A^+	609	394	−186	−688	795	0.47	0.46	272.0
				B^+	594	415	−199	−704	793	0.38	0.55	269.8
5	2.329(1)	2.262(2)	P−Se−Se−P = 118.7°	A^-	742	422	108	+477	634	0.99	0.01	424.5
		2.255(2)		A^+	751	423	76	−511	675	0.96	0.03	417.2
				B^-	703	452	−13	−590	716	0.64	0.30	381.2
				B^+	689	451	−30	−600	716	0.59	0.38	373.7

[a] Estimated errors in T_{11}, T_{22}, T_{33}, and ΔT are ±5 ppm; errors in δ_{iso} are ±0.2 ppm. Principal components of the effective dipolar/chemical shift tensor are defined as $T_{11} > T_{22} > T_{33}$. Isotropic chemical shift is given by $\delta_{iso} = (T_{11} + T_{22} + T_{33})/3$.

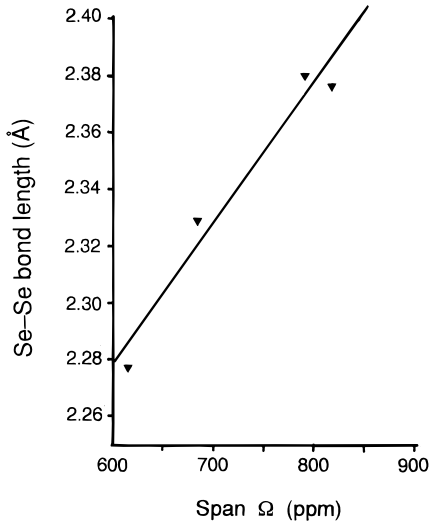

Figure 3. The relationship between the Se−Se bond length and the Ω for a series of bis(organothiophosphoryl) diselenides.

effect causes the shortening of the Se−Se bond and the lengthening of the P−Se distance. Moreover, the steric $S^1\cdots Se^4$ interaction in the $S^1{=}P{-}Se{-}Se^4{-}P{=}S$ unit results in the elongation of the P−Se bond when the diselenides are in the eclipsed conformation. As a result of these two effects, the P−Se distances are different: 2.299(2) Å for diselenide **1**, 2.218(1) Å for diselenide **2**, 2.223(2) and 2.230(2) Å for diselenide **3**, and 2.255(2) and 2.262(2) Å for diselenide **4** (Table 2).

We conclude that the ^{77}Se chemical shift parameters correspond to differences in the geometry of diselenides **1**, **3**, **4**, and **5**. It is known that the anisotropy parameters $\Delta\delta$ and Ω reflect the distortion of molecular structure from the ideal tetrahedral, while the asymmetry parameters η and κ reflect the asymmetry of the electron density distribution about the central atom. The local environment of selenium in bis(organothiophosphoryl) diselenides depends on the Se−Se−P, Se−P−S, and Se−P−O bond lengths and bond angles as well as p-electron lone pairs. The values of η and κ indicate that Se shielding is not localized at a particular bond but averaged out over the entire tetrahedron. The values of Ω for diselenides **1** and **5** (shorter Se−Se bond) are significantly smaller than for **3** and **4**. Figure 3 shows the linear relationship between the Se−Se distance and span Ω. It is therefore possible to correlate this parameter with the strength of the Se−Se bond and the P−Se−Se−P torsional angle.

The analysis of the isotropic chemical shifts is another source of structural information. The values of δ_{iso} for diselenides **3** and **4** are comparable (289 and 275 ppm), while the value for diselenide **5** is ca. 120 ppm downfield and for diselenide **1** almost 180 ppm. The isotropic chemical shift is the average of the sum of the principal elements of the effective dipolar/chemical shift tensor, so that more detailed information can be obtained by analyzing the tensor parameters. The most significant differences in the series of diselenides are for T_{33} (Table 2). The results indicate that T_{33} is aligned in the plane of the P−Se bond, and a linear correlation between T_{33} and phosphorus−selenium distance is apparent. The T_{33} parameters and Ω ($\Omega = T_{11} - T_{33}$) are also correlated.

Intramolecular Dynamics of *tert*-Butyl and Phenyl Groups. Riddel et al.[38−40] and Twyman and Dobson[41,42] have reported molecular motion in the solid state of the *tert*-butyl and phenyl groups. We have used high-resolution solid-state ^{13}C and ^{2}H NMR to study in detail the dynamics of alkyl/aryl groups bonded to the phosphorus. The ^{13}C dipolar dephasing experiment is a useful source of information on the molecular motion.[20] We have applied the commonly used sequence, where a variable dephasing period (interruption of proton decoupling) of duration t_1 is inserted at the end of the cross-polarization period and before data acquisition.[43] During the dephasing period, the magnetization of carbons is influenced by the heteronuclear dipolar interaction. According to the model of Demco et al.[44] the carbon atoms polarize at the relative rates $CH_{3(static)} > CH_2 > CH{=}CH_{3(rotated)} > C_{(nonprotonated)}$. In dipolar dephasing the rates of signal decay must obey this same relationship. For a dephasing time of 40 μs the resonances of the methine and methylene carbons are greatly attenuated.[45] A dephasing period of 40−120 μs gives a spectrum containing only lines from rotating methyls and quaternary carbons. All resonances in the ^{13}C CP/MAS spectrum of diselenide **1** at room temperature (not shown) can be unambiguously assigned. A plot of line intensities versus the dipolar dephasing delay is shown in Figure 4.

As predicted, the dynamics of *tert*-butyl and phenyl groups in diselenide **1** are very similar to that in disulfide **2**. The resonances of the *tert*-butyl quaternary carbon decay very slowly and for $t_1 = 400$ μs the signal can still be recorded. The resonances of the aromatic CH carbons disappear at $t_1 = 40$ ms. The *tert*-butyl methyl groups undergo very fast motion. For t_1 longer than 400 μs the intensity of the methyl lines is almost unchanged. The biexponential character of the decay curve shows that the motion of the *tert*-butyl group is rather complex.

Further information on the mode of the intramolecular dynamics of *tert*-butyl and phenyl groups was obtained using ^{2}H NMR. Line shape analysis of the static ^{2}H spectrum of

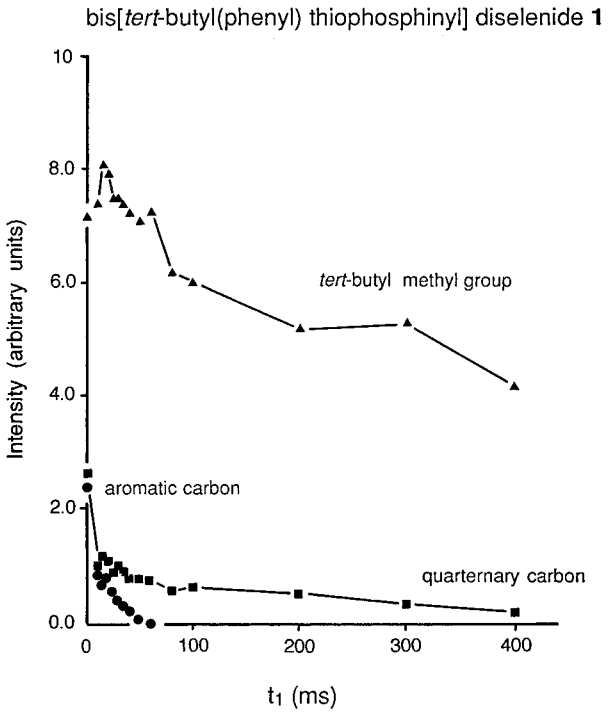

Figure 4. Plot of intensity versus t_1 for the *tert*-butyl methyl group, the quaternary carbon, and the aromatic carbon of diselenide **1**.

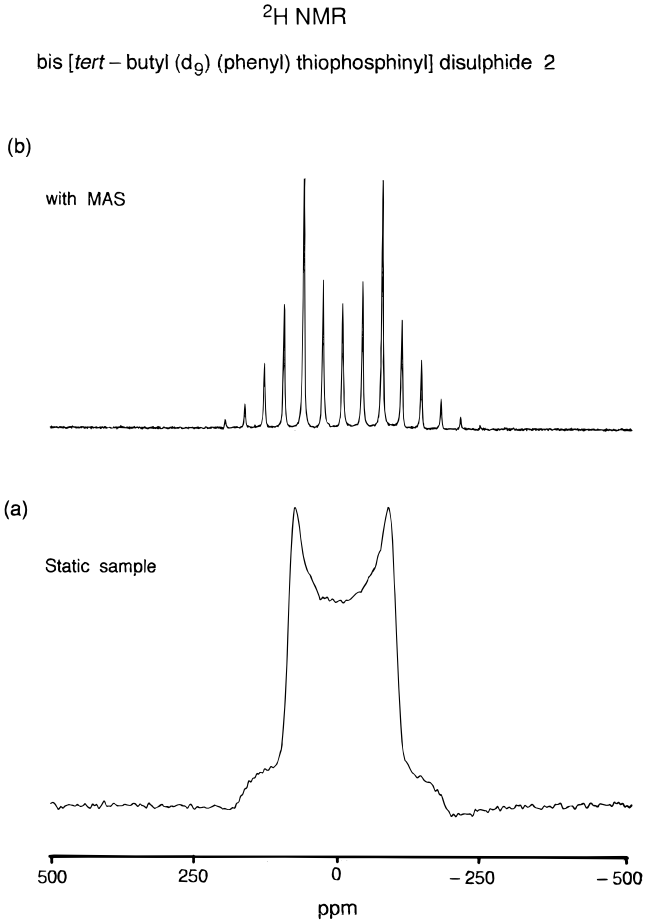

Figure 5. ^{2}H NMR spectra of bis[*tert*-butyl-d_9 (phenyl) thiophosphinyl] disulfide **2** acquired at 46.07 MHz: (a) static sample, (b) with MAS.

disulfide **2** (Figure 5a) indicates that rotation of the *tert*-butyl group about the C_3 axis (the C−C bond) is superimposed on the *tert*-butyl reorientation about $C_{3'}$ axis (the P−C bond) (Scheme 2).

SCHEME 2

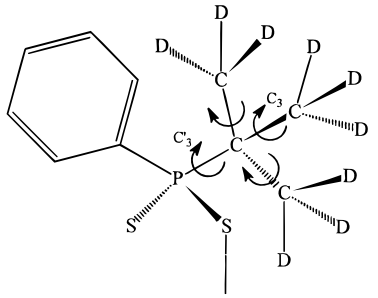

TABLE 3: Crystal Data and Experimental Details for Diselenide 1

molecular formula	$C_{20}H_{28}P_2S_2Se_2$
$F(000)$	1112.00
M	552.43
crystallographic system	monoclinic
space group	$C2/c$
a (Å)	20.424(2)
b (Å)	9.374(1)
c (Å)	12.907(1)
β (deg)	103.157(15)
V (Å^3)	2406.4(2)
Z	4
D_c (g/cm^3)	1.525(2)
μ (cm^{-1})	68.6
crystal dimensions (mm)	0.15, 0.40, 0.55
radiation, λ (Å)	Cu Kα, 1.541 84
diffractometer	Enraf-Nonius CAD4
scan mode	$\omega/2\theta$
scan width (deg)	$0.92 + 0.14 \tan\theta$
abs. correction min, max, av	0.7250, 0.9999, 0.9004
transmission min, max, av (%)	52.56, 99.97, 81.07
measured reflctns	2708
independent reflcns	2423
observed reflctns [$I > 3\sigma(I)$]	2351
R_{int}	0.0288
maximum 2θ (deg)	150
ranges h, k, l	0 to 25, −11 to 0, −16 to 16
parameters refined	118
weighting scheme	$\omega = [\sigma^2(F) + 0.003F^2]^{-1}$
$(\Delta/\sigma)_{max}$	0.0806
residual density max, min (eÅ^{-3})	0.547, −0.731
S	2.7919
$R\left(=\frac{\Sigma_{obs} - \Sigma_{calc}}{\Sigma_{obs}}\right)$	0.047

For a static methyl group QCC = 168 kHz with a quadrupole splitting of 126 kHz. Fast motion of a methyl group superimposed on the slow *tert*-butyl reorientation gives a motionally narrowed Pake doublet with a splitting of 42 kHz. If both motions are fast on the NMR time scale, the splitting is 14 kHz. The observed 10 kHz splitting is thus smaller than predicted even for fast motion around the C_3 and $C_{3'}$ axes, suggesting that a third motion may be superimposed on the two rotations. The most likely possibility is a low-amplitude lattice vibration of the molecular crystal. However, our ^{31}P CP/MAS studies in a wide temperature range exclude this possibility. An alternative explanation is that the methyl group or *tert*-butyl group deviates from tetrahedral geometry. The 10 kHz quadrupolar splitting was also reported for the *tert*-butyl group in the inclusion compound of thiourea/1,4-di-*tert*-butylbenzene.[46] ^{2}H MAS NMR experiments, more sensitive than static mesurements,[47,48] reveal that the splitting in disulfide **2** is 8 kHz (Figure 5b), consistent with that for a static measurement if the MAS rate (2 kHz) is taken into account.

We have used the same approach to study the dynamics of the phenyl group in bis[*tert*-butyl(phenyl-d_5)thiophosphinyl] dichalcogenides. The splitting in the spectrum of disulfide **2**

TABLE 4: Bond Lengths and Angles for Bis[*tert*-butyl(phenyl)thiophosphinyl] Diselenide 1

Se−Se[a]	2.277(1)	**C1−C2**	1.392(7)	**C5−C6**	1.388(9)
Se−P	2.299(2)	**C1−C6**	1.388(8)	**C7−C8**	1.517(9)
S−P	1.940(2)	**C2−C3**	1.404(8)	**C7−C9**	1.523(8)
P−C1	1.818(5)	**C3−C4**	1.358(10)	**C7−C10**	1.530(7)
P−C7	1.859(5)	**C4−C5**	1.362(13)		
P−Se−Se[b]	99.3(1)	**P−C1−C2**	121.9(4)	**C1−C6−C5**	119.7(6)
Se−P−S	114.0(1)	**P−C1−C6**	118.5(4)	**P−C7−C8**	111.5(4)
Se−P−C1	104.8(2)	**C2−C1−C6**	119.5(5)	**P−C7−C9**	108.7(4)
Se−P−C7	101.8(2)	**C1−C2−C3**	118.7(5)	**P−C7−C10**	107.1(4)
S−P−C1	112.3(2)	**C2−C3−C4**	121.2(6)	**C8−C7−C9**	111.0(5)
S−P−C7	114.6(2)	**C3−C4−C5**	119.7(7)	**C8−C7−C10**	109.4(5)
C1−P−C7	108.4(2)	**C4−C5−C6**	121.1(7)	**C9−C7−C10**	109.0(4)

[a] Bond lengths in angstroms. [b] Bond angles in degrees.

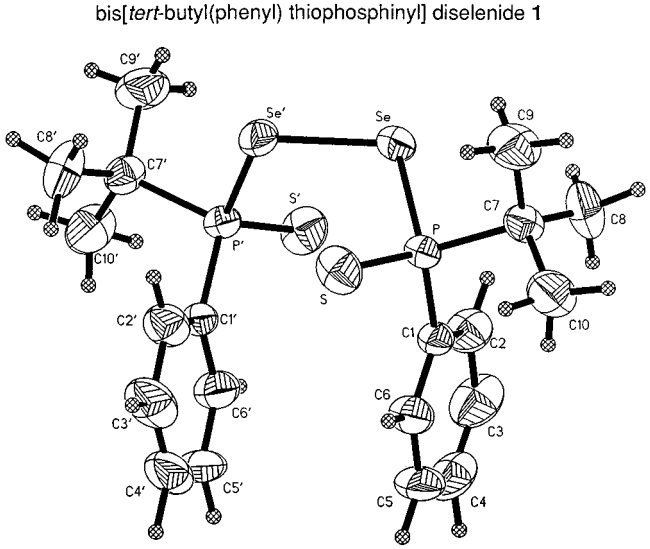

Figure 6. Thermal ellipsoidal view and atom numbering scheme of diselenide **1** in the asymmetric part of the unit cell. Half of the molecule is an asymmetric part of the unit cell; the primed atoms are from the symmetrical ($-x$, $2-y$, $1-z$) moiety.

spun at 3 kHz is 130 kHz, typical for a static phenyl group and fully consistent with the ^{13}C dipolar dephasing experiment.[49−51] Moreover, the T_1 discrimination experiment with the relaxation delay varied from 10 to 100 s shows a 50% gain in line intensity for the latter time delay. The very long ^{2}H relaxation time indicates the absence of motion of the phenyl group.

X-ray Diffraction. Experimental details and crystallographic parameters for diselenide **1** are given in Table 3 and selected geometric parameters in Table 4. Atomic coordinates and tables of bond lengths, bond angles, and torsional angles are submitted as Supporting Information. The ORTEP thermal ellipsoidal plot with the atom numbering scheme for bis[*tert*-butyl(phenyl)-thiophosphinyl] diselenide **1** is shown in Figure 6.

The crystal and molecular structures of diselenide **1** are very similar to those for disulfide **2**. Compound **1** crystallizes in the space group *C*2/*c* with a unit cell consisting of four molecules, half a molecule as an asymmetric unit. The bond lengths and angles calculated for the *tert*-butyl and phenyl groups are typical and do not greatly differ from the ideal values. The changes of the Se−Se and P−Se bond lengths as a function of S═P−Se−Se−P═S unit conformation have already been discussed. Why does the S═P−Se−Se−P═Se unit adopt *syn*−*syn* geometry if such conformation is unfavorable owing to the steric interactions? The answer comes from the analysis of molecular packing in the unit cell (Figure 7).

The phenyl groups bonded to phosphorus atoms in diselenide **1** are in parallel planes. In addition, the phenyls of the second molecule in the unit cell show similar orientation and the two molecules aligned "upside down" partially overlap. In consequence, we have four aromatic rings oriented "face-to-face". In the case of bis(organothiophosphoryl) dichalcogenides such "π-stacking" is not unusual, and bis[*tert*-butyl(phenyl)thiophosphinyl] disulfide **2** shows identical molecular packing.[20] We have constructed the unit cell (Figure 8) using the coordinates for bis(diphenylthiophosphinyl) disulfide which has the *syn*−*syn* geometry.[25] The similarity in molecular packing for the three compounds is apparent.

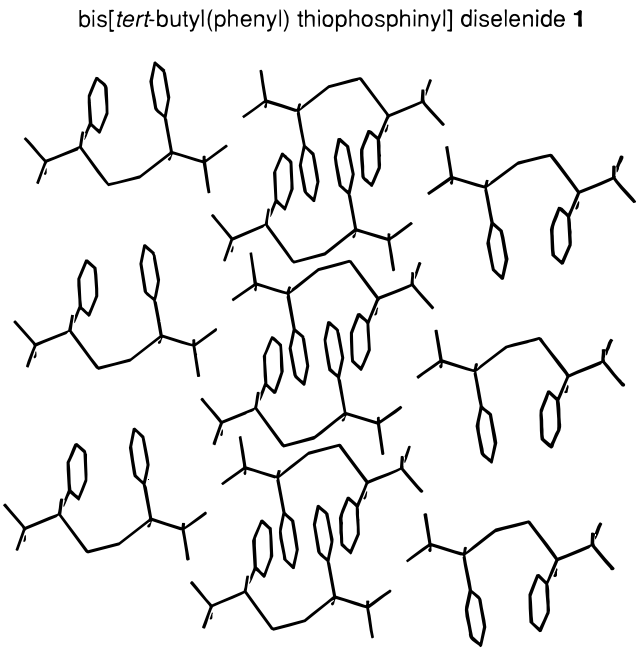

Figure 7. Unit cell of bis[*tert*-butyl(phenyl)thiophosphinyl] diselenide **1**.

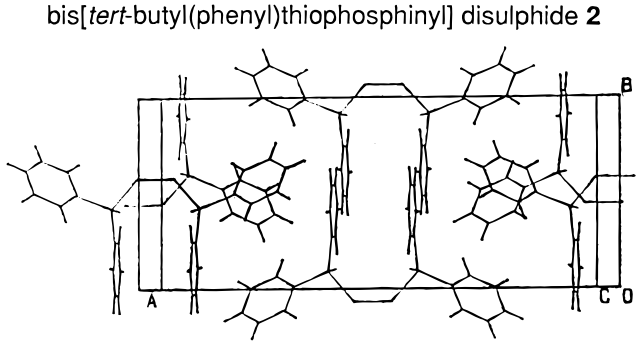

Figure 8. Unit cell of bis[*tert*-butyl(phenyl)thiophosphinyl] disulfide **2**.

The tendency to π-stacking in the systems under study can be explained using the "polar/π" approach which assumes electrostatic interaction between the positively charged σ-framework and the two negatively charged π-electron clouds.[10−13] Hunter and Sanders[10] have shown that the $\pi-\sigma$ attraction

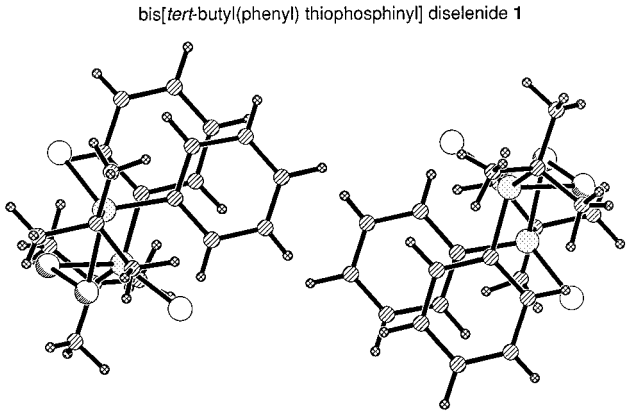

Figure 9. The structure of bis[*tert*-butyl(phenyl)thiophosphinyl] diselenide **1** showing the interaction of the phenyl groups.

SCHEME 3

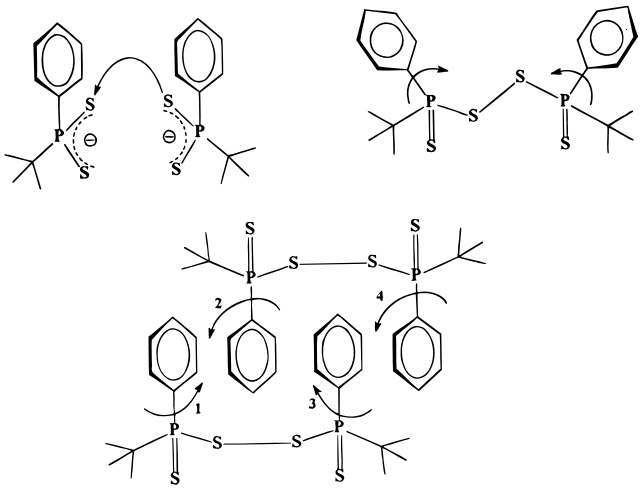

dominates in an offset π-stacked geometry. The phenyl rings of diselenide **1** and disulfide **2** are in the offset position (Figure 9).

The presence of strongly polarizing atoms has a major influence on the electrostatic interaction. An electron acceptor such as the dithiophosphoryl group is polarized so that the aromatic ring has a net positive charge and the substituent a net negative charge. The electron-acceptor interaction favors the face-to-face arrangement and thus the *syn*−*syn* geometry of phosphoroorganic dichalcogenides.[10] On the other hand, the phenyl group may be directly bonded to the phosphorus, as in bis[(−)menthyloxy(phenyl)thiophosphoryl] disulfide,[52] or via the oxygen atom, as in bis(diphenoxythiophosphoryl) disulfide,[20] which has the *anti*−*anti* geometry. These effects are also related to the substituents. The electron donor (oxygen) is polarized so that the aromatic ring has a net negative charge and the substituent a net positive charge. The electron-deficient π systems do not favor face-to-face stacking. A comparison of the *syn*−*syn* conformation for bis(diphenylthiophosphinyl) disulfide and *anti*−*anti* for bis(diphenoxythiophosphoryl) disulfide provides more evidence. In the case of bis[(−)menthyloxyphenylthiophosphoryl)] disulfide, the strong electron-acceptor effect of the dithiophosphoryl group is reduced because of the presence of the oxygen atom adjacent to the phosphorus. As a result, the S═P−S−S torsional angle is 150°.

The mechanism of chalcogen-chalcogen bond splitting is a challenging question (Scheme 3). At least three mechanisms leading to the *syn*−*syn* geometry in the disulfide/diselenide can be considered. The first assumes a preorganization of dithiophosphoric or thioselenophosphoric acids in such a manner that the $\pi-\pi$ interaction is a primary process and anticipates the oxidation of S−H (Se−H) to the dichalcogenide bond. The second assumes the formation of dichalcogenide bonds as a first step, and the aromatic−aromatic interaction which can be the driving force to the *syn*−*syn* geometry. It is interesting to consider the role of the second molecule of the bis[*tert*-butyl(phenyl)thiophosphinyl] dichalcogenide. The π-stacking can be considered as a four-step process where the interaction between the phenyl rings of molecules A and B in steps 1 and 2 affects the further aromatic−aromatic interactions (steps 3 and 4) (gear mechanism). There is no clear evidence in favor of one particular mechanism. However, the unusual selection in stereospecific synthesis of the P-epimeric of bis[(−)menthyloxyphenylthiophosphoryl)] disulfide and diselenide militates in favor of the first mechanism.[52,53]

Conclusions

Although relatively small (0.5−2 kJ/mol), the free energies of the aromatic $\pi-\pi$ interaction play an important role in the self-organization of crystal structures of phenyl substituted bis(organothiophosphoryl) dichalcogenides and determine the geometry around the S−S and Se−Se bonds. Inspection of published X-ray data reveals a tendency to adopt the planar *zigzag* array with *anti*−*anti* conformation for the S═P−X−X−P═S (X = S and Se) backbone. Although the *syn*−*syn* geometry is unfavorable because of the strong repulsive 1−4 interactions between the S and X atoms, the $\pi-\pi$ attractive interactions force the molecule to adopt the *syn* conformation. The changes of the geometry of the S−P−X−X unit cause significant changes to bond lengths and valence angles for the phosphorus and selenium centers. We confirm that the correlation between the anisotropy (and asymmetry) parameters and the S═P−X valence angle can be extended to diselenide systems and note the relationship between ^{77}Se chemical shift parameters and the strength of the Se−Se bond. There is a linear correlation between the span and the Se−Se distance, with smaller values of Ω corresponding to shorter Se−Se bonds. The ^{77}Se isotropic chemical shifts correspond to changes of S═P−Se−Se−P═S torsional angles. For shorter Se−Se bonds the values of Ω are smaller. The differences of δ_{iso} are mostly caused by the T_{33} principal elements of effective dipolar/chemical shift tensors, and we suggest that T_{33} is oriented in the plane of the P−Se bond. The ^{13}C dipolar dephasing experiment and line shape analysis of the Pake doublets measured by ^{1}H−^{2}H CP/MAS lead us to conclude that the phenyl rings are rigid and that π-stacking affects the intramolecular dynamics of the aromatic groups.

Acknowledgment. We are grateful for the Polish Committee for Scientific Research (KBN) for support (Grant 3TO9A11612).

Supporting Information Available: Tables of atomic coordinates, isotropic and anisotropic temperature factors, and bond lengths and bond angles, as well as torsional angles, for **1** (4 pages). Ordering information is given on any current masthead page. Tables of atomic coordinates and thermal parameters have been deposited with the Crystallographic Data Centre, Cambridge University Chemical Laboratory, Cambridge CB2 1EW, U.K.

References and Notes

(1) (a) Jorgensen, W. L.; Severance, D. L. *J. Am. Chem. Soc.* **1990**, *112*, 4768. (b) Hunter, C. A. *Chem. Soc. Rev.* **1994**, *23*, 101 and references therein.

(2) (a) Desiraju, G. R.; Gavezzotti, A. *J. Chem. Soc., Chem. Commun.* **1989**, 621. (b) Desiraju, G. R.; Gavezzotti, A. *Acta Crystallogr.* **1989**, *B45*, 473.

(3) Burley, S. K.; Petsko, G. A. *Adv. Protein Chem.* **1988**, *39*, 125 and references therein.
(4) (a) Suzuki, M.; Ohmor, H.; Kajtar, M.; Szetjtl, J.; Vikmon, M. *J. Inclusion Phenom. Mol. Recognit.* **1994**, *18*, 225. (b) Pirkle, W. H.; Selness, S. R. *J. Org. Chem.* **1995**, *60*, 3252.
(5) Evans, D. A.; Chapman, K. T.; Hung, D. T.; Kawaguchi, A. T. *Angew. Chem., Int. Ed. Engl.* **1987**, *26*, 1184 and references therein.
(6) Saenger, W. *Principles of Nucleic Acid Structure*; Springer-Verlag: New York, 1984; pp 132−140.
(7) Desiraju, G. R. *Angew. Chem., Int. Ed. Engl.* **1995**, *34*, 2311.
(8) Laatikainen, R.; Ratilainen, J.; Sebastian, R.; Santa, H. *J. Am. Chem. Soc.* **1995**, *117*, 11006.
(9) Shetty, A. S.; Zhang, J.; Moore, J. S. *J. Am. Chem. Soc.* **1996**, *118*, 1019 and references therein.
(10) Hunter, C. A.; Sanders, J. K. M. *J. Am. Chem. Soc.* **1990**, *112*, 5525.
(11) Cozzi, F.; Siegel, J. S. *Pure Appl. Chem.* **1995**, *67*, 683.
(12) Cozzi, F.; Cinquini, M.; Annunziata, R.; Siegel, J. S. *J. Am. Chem. Soc.* **1993**, *115*, 5330.
(13) Cozzi, F.; Cinquini, M.; Annunziata, R.; Dwyer, T.; Siegel, J. S. *J. Am. Chem. Soc.* **1992**, *114*, 5729.
(14) Potrzebowski, M. J. *Magn. Reson. Chem.* **1992**, *30*, 35.
(15) Potrzebowski, M. J. *J. Chem. Soc., Perkin Trans. 2* **1993**, 63.
(16) Potrzebowski, M. J.; Grossmann, G.; Blaszczyk, J.; Wieczorek, M. W.; Sieler, J.; Knopik, P.; Komber, H. *Inorg. Chem.* **1994**, *33*, 4688.
(17) Potrzebowski, M. J. *Magn. Reson. Chem.* **1995**, *35*, 8.
(18) Potrzebowski, M. J.; Blaszczyk, J.; Wieczorek, M. W. *J. Org. Chem.* **1995**, *60*, 2549.
(19) Potrzebowski, M. J.; Michalski J. In *Phosphorus-31 NMR. Spectral Properties in Compound Characterization and Structural Analysis*; Quin, L. D., Verkade, J. G., Eds.; VCH: New York, 1994; pp 413−426.
(20) Knopik, P.; Luczak, L.; Potrzebowski, M. J.; Michalski, J.; Blaszczyk, J.; Wieczorek, M. J. *J. Chem. Soc., Dalton Trans.* **1993**, 2749.
(21) Creighton, S. *BioEssays* **1988**, *8*, 57.
(22) Huxtable, R. J. Biochemistry of Sulphur; Plenum: New York, 1981.
(23) (a) Burunda, T.; Gallacher, A. C.; Pinkerton, A. A. *Acta Crystallogr.* **1991**, *C47*, 1414. (b) Gallacher, A. C.; Pinkerton, A. A. *Acta Crystallogr.* **1992**, *C48*, 2085.
(24) (a) Lawton, S. *Inorg. Chem.* **1970**, *9*, 2269. (b) Yadaw, J. S.; Bohra, R.; Mehrota, R. K.; Rai, A. K.; Srivastava, G. *Acta Crystallogr.* **1983**, *C45*, 308. (c) Potrzebowski, M. J.; Reibenspies, J. H.; Zhong, Z. *Heteroat. Chem.* **1991**, *2*, 455.
(25) Gallacher, A. C.; Pinkerton, A. A. *Acta Crystallogr.* **1993**, *C49*, 1793.
(26) WIN-MAS Program, version 940108; Bruker-Franzen Analytik GmbH: Bremen, 1994.
(27) Jeschke, G.; Grossman, G. *J. Magn. Reson.* **1993**, *A103*, 323.
(28) Herzfeld, J.; Berger, A. *J. Chem. Phys.* **1980**, *73*, 6021.
(29) Mason, J. *Solid State Nucl. Magn. Reson.* **1993**, *2*, 285.
(30) Schagen, J. D.; Straver, L.; van Meurs, F.; Williams, G. *CAD4 Diffractometer Operator's Manual*, Version 5.0; Enraf-Nonius: Delft, The Netherlands, 1989.
(31) Frenz, B. A. *SDP-Structure Determination Package*; Enraf-Nonius: Delft, The Netherlands, 1984.
(32) *SHELXTL PC*, Release 4.1.; Siemens Analytical X-ray Instruments, Inc. Madison, WI 53719, 1990.
(33) *International Tables for X-ray Crystallography*; Kynoch Press: Birmingham, U.K., 1974.
(34) Cambridge Crystallographic Data Centre, 12 Union Road, Cambridge CB2 1EW, U.K.
(35) Collins, M. J.; Ratclieff, C. I.; Ripmeester, J. A. *J. Magn. Reson.* **1986**, *68*, 172.
(36) Zilm, K. W.; Grant, D. M. *J. Am. Chem. Soc.* **1981**, *103*, 2913.
(37) Potrzebowski, M. J.; Blaszczyk, J.; Wieczorek, M. W.; Baraniak, J.; Stec, W. J. *J. Chem. Soc., Perkin Trans. 2.* Submitted for publication.
(38) Riddell F. G.; Rogerson, M. J. *Chem. Soc., Perkin Trans. 2* **1996**, 493.
(39) Riddell, F. G.; Arumugam, S.; Harris, K. D. M.; Rogerson M. *J. Am. Chem. Soc.* **1993**, *115*, 1881.
(40) Riddell, F. G.; Bernáth, G.; Fûlöp, F. *J. Am. Chem. Soc.* **1995**, *117*, 2327.
(41) Twyman, J. M.; Dobson, C. M. *J. Chem. Soc., Chem. Commun.* **1988**, 786.
(42) Twyman, J. M.; Dobson, C. M. *Magn. Reson. Chem.* **1990**, *28*, 163.
(43) Alla, M.; Lippmaa, E. *Chem. Phys. Lett.* **1976**, *37*, 260.
(44) Demco, D. E.; Tegenfeld, J.; Waugh, J. S. *Phys. Rev. B* **1975**, *11*, 4133.
(45) Opella, S. J.; Frey, M. H. *J. Am. Chem. Soc.* **1979**, *37*, 260.
(46) Penner, G. M.; Polson, J. M.; Ferguson, G.; Kastner, B. *J. Phys. Chem.* **1992**, *96*, 5121.
(47) Kristensen, J. H.; Bildsøe, H.; Jakobsen, H. J.; Nielsen, N. Ch. *J. Magn. Reson.* **1991**, *92*, 443.
(48) Schadt, R. J.; Dong, R. Y.; Günther, E.; Blümich, B. *J. Magn. Reson.* **1991**, *92*, 443.
(49) Vold, R. R. In *Nuclear Magnetic Resonance Probes of Molecular Dynamics*; Tycko, R. Ed.; Kluwer Academic Publishers: Dordrecht, 1994; pp 27−112.
(50) Spiess, H. W. *Adv. Polym. Sci.* **1985**, *66*, 23.
(51) Griffin, R. G. *Methods Enzymol.* **1981**, *72*, 108.
(52) Lopusinski, A.; Luczak, L.; Michalski, J.; Koziol A. E.; Gdaniec, M. *J. Chem. Soc., Chem. Commun.* **1991**, 455.
(53) Lopusinski, A.; Luczak, L.; Michalski, J. *Heteroat. Chem.* **1995**, *4*, 365.